Generation of Terahertz Surface Plasmon Polaritons Using Nondiffractive Bessel Beams with Orbital Angular Momentum

B. A. Knyazev,[1,2,*] Yu. Yu. Choporova,[1,2] M. S. Mitkov,[1,2,3] V. S. Pavelyev,[4,5] and B. O. Volodkin[4]
[1]Budker Institute of Nuclear Physics SB RAS, 630090 Novosibirsk, Russia
[2]Novosibirsk State University, 630090 Novosibirsk, Russia
[3]Novosibirsk State Technical University, 630073 Novosibirsk, Russia
[4]Samara State Aerospace University, 443086 Samara, Russia
[5]Image Processing Systems Institute RAS, 443001 Samara, Russia
(Received 17 March 2015; published 14 October 2015)

Bessel vortex beams with topological charges of $l = \pm 1$ and $l = \pm 2$ were produced in the terahertz spectral range from a free electron laser Gaussian beam ($\lambda = 141$ μm) transformed using silicon binary diffractive optical elements. The spatial characteristics of the beams were obtained using a microbolometer array. A radius to path length ratio of 1:100 was achieved for nondiffractive beams with the average power of 30 W. Surface plasmon polaritons (SPPs) on gold–zinc-sulphide–air interfaces were generated due to diffraction of vortex beams on a sample edge. A new effect, a dependence of the efficiency of SPP generation on the direction of the azimuthal component of incident-radiation Poynting vector, was revealed.

DOI: 10.1103/PhysRevLett.115.163901 PACS numbers: 42.60.Jf, 41.60.Cr, 42.50.Tx, 73.20.Mf

Plasmonics [1] and photonics [2] are today the most rapidly developing areas of modern optics. Among the important domains in plasmonics is the study of the generation and transport of surface plasmon polaritons (SPPs) and the development of methods for manipulating them. Although surface plasmon polaritons have been studied for a century, and their properties are well examined [1,3,4], the interest in them has increased in recent years, in particular in connection with the development of nano-optics and the prospect of their practical application [5–7]. The research in the domain of the generation and use of beams with orbital angular momentum [8–10], which is usually referred to as the field of photonics, arose relatively recently, and this area of research is gradually expanding.

These two domains did not intersect until 2009, when the generation of surface optical vortices via internal total reflection was suggested [11]. Surface plasmon vortex generation with a plasmonic vortex lens, a specific curved slit pattern on a thin metal film, was experimentally demonstrated using laser radiation with circular polarization [12]. Later [13], surface plasmon waves with phase singularity were generated just by normal incidence of a free wave vortex beam on a thin silver film. An experiment on the transformation of a free vortex beam into unidirectional SPPs, using a holographic coupler consisting of curved fork-shaped grooves, was described in Ref. [14]. All the above experiments were carried out in the visible range. In this Letter we examine another experimental configuration to convert vortex beams into SPPs using monochromatic terahertz radiation. Characteristics of terahertz plasmons, which differ in many aspects from those in the visible range, and possible fields of applications of terahertz SPPs were recently discussed in Ref. [15].

To date, we know three experiments on the generation of vortex beams in the terahertz range. He *et al.* [16] generated and studied a terahertz vortex beam with a *V*-shaped antenna array using a broadband terahertz source. Miyamoto *et al.* [17] generated vortex beams at 2 and 4 THz using a spiral phase plate (not Fresnel zone plate) made of Tsurupica and a tunable monochromatic source of radiation. Imai *et al.* [18] demonstrated another technique for the generation of terahertz vortex beams. Using a sectioned achromatic quarter-wave plate coupled to a wire polarizer, they converted a radially polarized broadband terahertz beam into a broadband vortex beam. In all these papers the authors showed that the beams generated could be approximated well with the Laguerre-Gaussian function.

In this Letter we report on the formation of terahertz Bessel vortex beams, the investigation of their characteristics, and the generation of surface plasmon polaritons via diffraction of the vortex beams on the edge of a metal-dielectric interface. Some details that are useful for better understanding the content of the Letter are presented in the Supplemental Material [19]. The Novosibirsk free electron laser (NovoFEL) was used as a source of radiation [26,27]. The NovoFEL, the wavelength of which can be tuned to any wavelength between 90 and 240 μm with the halfwidth $\Delta\lambda/\lambda \leq 0.01$, generates linearly polarized radiation as a continuous stream of 100 ps pulses at a repetition rate of 5.6 MHz. It is worth noting here we hardly could perform this work without a high-power monochromatic source of terahertz radiation. To separate, in space, the bulk diffracted wave and surface plasmon (see the last part of the Letter) we had to use a cylindrically curved metal-dielectric interface for SPP transport to the detector. The radiation losses because of the emission by a plasmon travelling

along a curved interface [28] substantially decrease intensity of the plasmon at the sample end and, consequently, the intensity of the wave emitted into the free space. Despite the rather high sensitivity of the microbolometer matrix [29], the signal turns out to be only 10 times higher as compared with the noise, whereas the average power of the input radiation emitted by the NovoFEL [26] is not less than several tens of watts.

Vortex beams with $l = \pm 1$ and $l = \pm 2$ at the wavelength $\lambda = 141$ μm were formed using silicon binary phase plates with a spiral configuration of zones [see Fig. 1(a)]. As a prototype of this plate, we can mention the amplitude zone plates with a spiral configuration of Fresnel zones applied in Ref. [30] to the generation of vortex beams in the visible range. Our diffraction elements can be classified as a phase spiral Fresnel plates. The diameter of the plates was equal to 38 mm. The technology applied for fabrication of the plates was described in Ref. [31].

A linearly polarized NovoFEL Gaussian beam with a waist of 15.2 mm illuminates a zone plate and, after passing the plate, turns into a vortex beam at a distance z of about 110 mm [Fig. 1(b)]. Two polarizers, which are situated before the plate and are not shown in the picture, are used for changing the polarization direction of the vortex beam. All the images are presented for an observer watching along the z axis. Images of the beam are recorded in real time using a 320×240 microbolometer array [21,29] the physical size of which is 16.36×12.24 mm^2. The beam cross sections differ for different topological charges, but

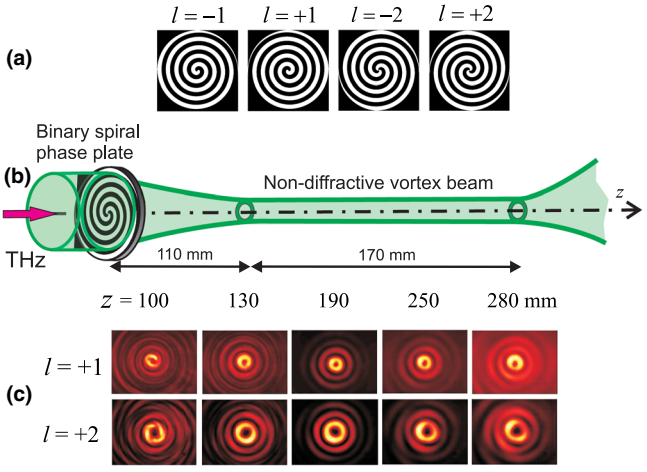

FIG. 1 (color online). Generation of beams with orbital angular momentum. (a) The phase functions of the elements which form vortex beams with topological charges of $l = \pm 1$ and $l = \pm 2$. The white color corresponds to a phase value of π and the black color to a phase value of zero. (b) Experimental setup. Here and below we use the right-handed coordinate system, and the phase angle grows up in the clockwise direction. The binary phase spiral-zone plates are set at $z = 0$. (c) Experimentally observed intensity distributions of the beams with $l = +1$ and $l = +2$ vs distance for $\lambda = 141$ μm.

do not depend on the incident beam polarization and sign of the topological charge. We wrote a code in the Fresnel-Kirchhoff approximation for simulation of the beam amplitude and phase characteristics. The code showed excellent agreement between the experimentally observed and simulated patterns for these and subsequent experiments.

The beams formed with the plates turned out to be nondiffractive [Fig. 1(c)]. We found that the radial distributions of beam intensities were well approximated with Bessel functions of the first kind of order $|l|$. At a distance $z = 110$–260 mm, where the vortex beams are completely formed, the simulations and experiments show that the beam amplitude and phase can be written as

$$E(r, \varphi, z) = E_0 J_{|l|}(\alpha r) e^{-i\omega t + i(kz + l\varphi)}, \quad (1)$$

where $k = 2\pi/\lambda$; $r = \sqrt{x^2 + y^2}$; φ is the azimuthal angle, and α is the scaling factor. The diameters of the first rings are 1.7 mm and 3.2 mm for the beams with $l = \pm 1$ and $l = \pm 2$, respectively, and do not change from $z = 110$ to $z = 260$ mm. Nevertheless, the beam power (which is proportional to surface integrals over the frame) decreases with the distance. This means that the beam wave front gradually turns into a spherical one. A numerical calculation of phase distribution in the beam as a function of z confirms that.

We have proved this assumption experimentally via the interference of the vortex beams with a collinear Gaussian beam in the Mach-Zehnder interferometer [Fig. 2(a)] at a distance of $z = 260$ mm. In this case a spiral-like interference pattern [32] is expected. The experimentally observed and simulated patterns [Figs. 2(b) and 2(c)] are in excellent agreement and clearly show the sign of topological charge. It is worth noting that noncollinear beams produce [Fig. 2(d)] well-known forklike interference fringes [9,30,32].

The above interference patterns are often used as evidence of a beam twist. Apparently, a beam twist can be detected in a simpler way, using classical diffraction experiments. We applied Young's double-slit diffraction and observed, as expected, dogleg-shaped strips [33]. The value and sign of the topological charge of the beam were easily retrieved from the observed fringe shapes, which we do not show here for space considerations. Vortex beam diffraction on a half-plane [Fig. 3(a)] is an even simpler diffraction experiment, which also is in direct relationship with our subsequent experiments with surface plasmon polaritons. Simulations of diffraction patterns [Fig. 3(b)] show that for a hypothetic beam, the intensity distribution of which is the same as that of the vortex beam but without twist ($l = 0$), the diffraction pattern is symmetrical relative to the x axis, whereas for the vortex beams it unexpectedly turns out to be nonsymmetric. Experiments and simulations

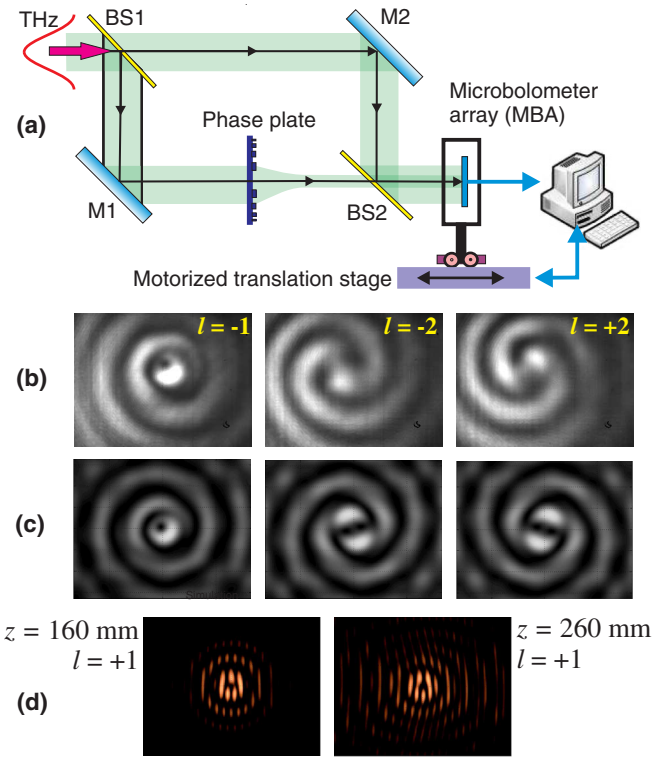

FIG. 2 (color online). Interference of vortex beams with a reference beam in the Mach-Zehnder interferometer. (a) Experimental schematic. Experimentally observed (b) and simulated (c) interference patterns for beams with different topological charges at a distance of 260 mm; the vortex and reference beams are collinear. (d) Calculated patterns for the interference of vortex beam with a reference Gaussian beam incident at an angle of 0.2 rad. The crooked fringes for $z = 260$ mm evidence the vortex beam wave front sphericity.

with a knife-edge obstacle for the vortex beams give the same results.

Now we come to the final subject of this Letter, i.e., the generation of terahertz surface plasmon polaritons using vortex beams. In plasmonic devices in the visible spectral range, one often applies SPP transmission along a metal-air interface. With increasing wavelength coupling of the SPPs to the metal surface weakens. The mainstream for up-to-date SPP terahertz plasmonics is using surfaces with designer metastructures [1,34] that provide better coupling of SPP. However, using thin dielectric films deposited onto metal surfaces substantially increases the SPP coupling, which can be employed in planar plasmonic devices. The large propagation length of terahertz plasmons [35] (a few centimeters as compared with tens of micrometers for the visible light) may be beneficial to such applications.

We applied the end-fire coupling technique (see Ref. [36] and references in it), i.e., the diffraction of an incident beam at the edge of a conductor-dielectric interface, to launch surface plasmons. The vortex beams [Fig. 3(c)] impinge on a cylindrical sample face. The microbolometer array

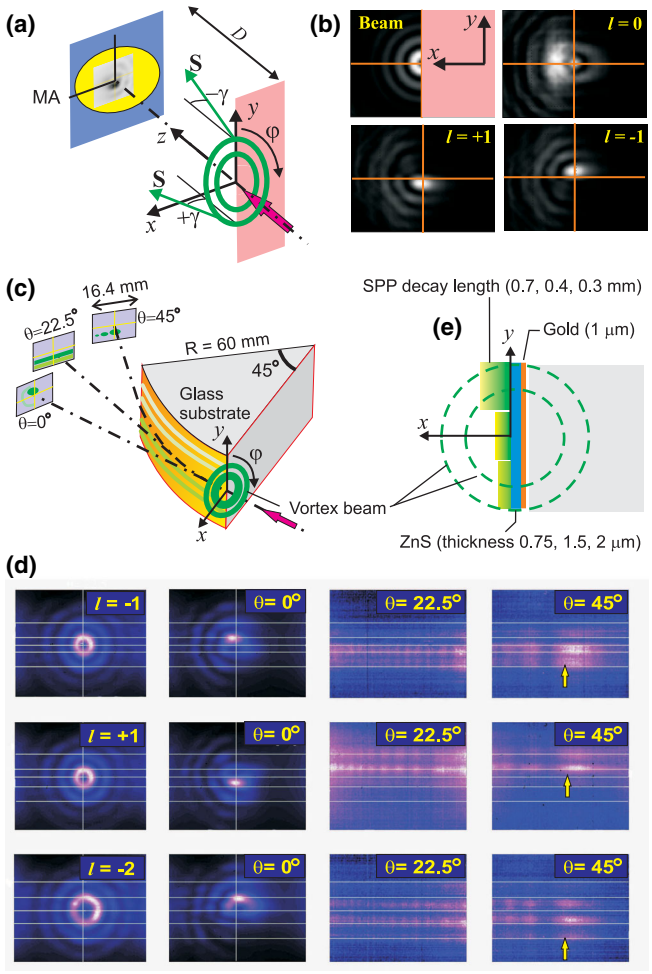

FIG. 3 (color online). (a) Experimental configuration for study of diffraction on a knife-edge obstacle; **S** is the Poynting vector. (b) Simulated diffraction patterns ($z = 150$ mm and $D = 60$ mm) for the beams with topological charges $l = 0, +1$, and -1, the intensity distributions of which are identical to those of our vortex beam. (c) Surface plasmon polariton generation by the vortex beams. (d) Images recorded for beams with different topological charges; the ZnS thickness is 1.5 μm; the distance from the input face to the array is 70 mm. (e) Schematic drawing showing the SPP decay length in air near gold-ZnS-air interfaces for three ZnS thicknesses in comparison with the diameters of the first two rings of the beams with $l = \pm 1$. Surface plasmons were generated only when the incident beam was p polarized (the electric vector of the wave laid along the x axis).

records the diffraction pattern (in a position corresponding to $\theta = 0°$), the tangentially scattered radiation ($\theta = 22.5°$), and the free wave produced by a plasmon diffracted at the end of the cylindrical surface ($\theta = 45°$). The probability of SPP generation in our case is expected to be proportional to the overlap integral between the intensity distribution of the vortex beams, see the left column of Fig. 3(d), and the SPP decay length [see Fig. 3(e)]. Since the radii of the vortex beam rings are greater than the decay lengths, one may expect the SPPs to be generated near the cross sections of

the sample surface with the vortex beam rings. The strips (green in the online version of the Letter) on the cylindrical surface show the anticipated SPP traces, but experiments reveal that the efficiency of SPP generation depends on the direction of the beam twist.

The diffraction of the vortex beams on the cylindrical sample [the second column in Fig. 3(d)] is nonsymmetric, which is in agreement with the simulations [Fig. 3(b)]. It is identical to the diffraction pattern of the vortex beams on the knife-shaped edge (see Supplemental Material [19]), but radically differs from the diffraction of conventional beams. Images recorded by the array placed near the output end of the cylindrical surface ($\theta = 45°$) clearly testify that surface plasmons that have passed the curved surface and are diffracting at the output edge produce free waves, marked with yellow arrows in the forth column of Fig. 3(d). The patterns agree well with the diffraction patterns obtained when a SPP is diffracted on the tail edge of a plane surface. The reliability of this diagnostic technique was proved in Refs. [35,37].

The intensities of these free waves are as small as $\sim 1/1000$ of the incident wave intensity, which is close to the lower limit of the microbolometer array sensitivity. For this reason, using the high-power FEL was critically important in our experiments. The radiation losses of SPPs traveling along the cylinder surface are well seen in the images shown in the third column of Fig. 3(d). The interference fringes seen in the images at the angle $\theta = 22.5°$ are, apparently, artifacts, appearing because of the Fabri-Perot effect inside the microbolometer array. That was corroborated using an optoacoustic detector. Comparing the intensities of all radiation components, we roughly estimate the efficiency of the SPP generation to be, at least, a few percent.

The most remarkable feature in the SPP generation with vortex beams is its asymmetry with respect to the optical axis. As we already noted, if the diffraction maximum appears on different sides for different signs of topological charges, SPPs are also generated asymmetrically, but on the sides opposite to the diffraction maxima. If one looks at Fig. 3(a), the only phenomenological explanation to this fact may be the difference in the Poynting vector direction for the left and right cross sections of vortex beam rings with the sample edge. If the Pointing vector is directed upward from the surface, we observe the diffraction maximum. In the contrary case, SPPs are generated on the side where the Pointing vector is directed into the surface. This "rule" works well for $l = \pm 1$. For $l = \pm 2$ we observe the same tendency, but an additional more weaker plasmon may appear on the opposite side of the optical axis. There may be some qualitative explanations for this phenomenon, but we prefer to state the fact and leave this problem for further consideration. We are planning to study the phenomenon in more detail in the next experimental session at the NovoFEL.

In conclusion, we have described a novel system for the generation of terahertz beams with orbital angular momentum. Using the radiation of the Novosibirsk free electron laser we have formed terahertz Bessel beams with different topological charges the average power of which reached about 30 W. The beams passed distances $\Delta z/r \sim 100$, where r is the first ring radius, which in combination with the high power of the beam is promising as concerns remote sensing applications and transmission radioscopy of extensive objects. We have demonstrated the generation of surface plasmon polaritons by vortex beams diffracted on the edge of a metal-dielectric interface, the efficiency surprisingly depending on the local Poynting vector direction. This effect, which still requires further investigation, might be applied to, for example, the creation of an optical switch in future terahertz photonic devices.

Operation of the user station "Terarad" belonging to the Novosibirsk State University, was supported by the Ministry of Education and Science of the Russian Federation (MES RF). The diffractive optical elements (DOEs) were designed with the support of MES RF (project 1879) and fabricated with the support of RFBR Grant No. 13-02-97007. The equipment for characterization of DOEs was developed with the support of Russian Science Foundation (project 14-50-00080). The study of beams with orbital angular momentum was supported by RFBR Grant No. 15-02-06444. The experiments were carried out with the application of equipment belonging to the Siberian Center of Synchrotron and Terahertz Radiation. The authors are grateful to G. N. Kulipanov and N. A. Vinokurov for interest in this work and stimulating discussions, and to the NovoFEL team for the invaluable support of the experiments. B. A. K. is indebted to V. G. Serbo, who attracted his attention to the vortex beams, and to A. K. Nikitin, who supplied us with the samples.

*ba_knyazev@phys.nsu.ru

[1] S. A. Maier, *Plasmonics: Fundamentals and Applications* (Springer, New York, 2007).
[2] *Photonics: Scientific Foundations, Technology and Applications*, edited by D. L. Andrews (John Wiley & Sons, New York, 2015), Vol. 1.
[3] G. N. Zhizhin, M. A. Moskaleva, E. V. Shomina, and V. A. Yakovlev, *Surface Polaritons. Electromagnetic Waves at Surfaces and Interfaces* (North-Holland, Amsterdam, New York, 1982), Chap. 3.
[4] H. Raether, *Surface Plasmons on Smooth and Rough Surfaces and on Grating* (Springer-Verlag, Berlin, 1988).
[5] L. Novotny and B. Hecht, *Principles of Nano-optics* (Cambridge University Press, Cambridge, England, 2006).
[6] W. L. Barnes, A. Dereux, and T. W. Ebbesen, Nature (London) **424**, 824 (2003).
[7] A. V. Zayats and I. I. Smolyaninov, Opt. A: Pure Appl. Opt. **5**, S16 (2003).

[8] L. Allen, M. W. Beijersbergen, R. J. C. Spreeuw, and J. P. Woerdman, Phys. Rev. A **45**, 8185 (1992).
[9] A. M. Yao and M. J. Padgett, Adv. Opt. Photonics **3**, 161 (2011).
[10] *Twisted Photons, Application of Light with Orbital Angular Momentum*, edited by J. P. Torres and L. Torner (Wiley-VCH Verlag & Co. KGaH, Weinheim, Germany, 2011).
[11] V. E. Lembessis, M. Babiker, and D. L. Andrews, Phys. Rev. A, **79**, 011806(R) (2009).
[12] H. Kim, J. Park, S.-W. Cho, S.-Y. Lee, M. Kang, and B. S. Lee, Nano Lett. **10**, 529 (2010).
[13] P. S. Tan, G. H. Yuan, Q. Wang, N. Zhang, D. H. Zhang, and X.-C. Yuan, Opt. Lett. **36**, 3287 (2011).
[14] P. Genevet, J. Lin, M. A. Kats, and F. Capasso, Nat. Commun. **3**, 1278 (2012).
[15] D. M. Mittleman, Nat. Photonics **7**, 666 (2013).
[16] J. X. He, X. Wang, D. Hu, J. Ye, S. Feng, Q. Kan, and Y. Zhang, Opt. Express **21**, 20230 (2013).
[17] K. Miyamoto, K. Suizu, T. Akiba, and T. Omatsu, Appl. Phys. Lett. **104**, 261104 (2014).
[18] R. Imai, N. Kanda, T. Higuchi, K. Konishi, and M. Kuwata-Gonokami, Opt. Lett. **39**, 3714 (2014).
[19] See Supplemental Material at http://link.aps.org/supplemental/10.1103/PhysRevLett.115.163901 containing following sections: Coordinate system; Design and fabrication of spiral zone plates; Numerical simulations; Detector of terahertz radiation; Votex beams: Experiment and simulations; Detection of topological charge value and sign via Young's diffraction; Diffraction of vortex beams on a half-plane; Detection of surface plasmon polaritons via their diffraction on sample end, which includes Refs. [20–25].
[20] *Computer Design of Diffractive Optics*, edited by V. A. Soifer (Cambridge International Science Publishing Ltd. & Woodhead Pub. Ltd., Cambridge, 2012), p. 896.
[21] M. A. Dem'yanenko, D. G. Esaev, I. V. Marchishin, V. N. Ovsyuk, B. I. Fomin, B. A. Knyazev, and V. V. Gerasimov, Optoelectronics, Instrumentation and Data Processing **47**, 508 (2011).
[22] O. Matula, A. G. Hayrapetyan, V. G. Serbo, A. Surzhykov, and S. Fritzsche, J. Phys. B **46**, 205002 (2013).
[23] V. V. Kotlyar, A. A. Kovalev, R. V. Skidanov, and V. A. Soifer, J. Opt. Soc. Am. A **31**, 1977 (2014).
[24] Y. Ismail, N. Khilo, V. Belyi, and A. Forbes, J. Opt. **14**, 085703 (2012).
[25] O. Emile and J. Emile, Appl. Phys. B **117**, 487 (2014).
[26] B. A. Knyazev, G. N. Kulipanov, and N. A. Vinokurov, Meas. Sci. Technol. **21**, 054017 (2010).
[27] G. N. Kulipanov, E. G. Bagryanskaya, E. N. Chesnokov, Y. Y. Choporova, V. V. Gerasimov, Y. V. Getmanov, S. L. Kiselev, B. A. Knyazev, V. V. Kubarev, S. E. Peltek, V. M. Popik, T. V. Salikova, M. A. Scheglov, S. S. Seredniakov, O. A. Shevchenko, A. N. Skrinsky, S. L. Veber, and N. A. Vinokurov, IEEE Trans. Terahertz Sci. Technol. **5**, 798 (2015).
[28] B. A. Knyazev, V. V. Gerasimov, V. O. Gorovoy, V. S. Cherkassky, G. N. Kulipanov, I. A. Kotelnikov, A. K. Nikitin, and G. N. Zhizhin, in *Proc. 39th Internat. Conf. on Infrared, Millimeter and Terahertz Waves, Tucson, USA* (IEEE, New York, 2014). p. 595–596.
[29] M. A. Demyanenko, D. G. Esaev, B. A. Knyazev, G. N. Kulipanov, and N. A. Vinokurov, Appl. Phys. Lett. **92**, 131116 (2008).
[30] R. N. Heckenberg, R. McDuff, C. P. Smith, and A. G. White, Opt. Lett. **17**, 221 (1992).
[31] A. N. Agafonov, B. O. Volodkin, S. G. Volotovsky, A. K. Kaveev, B. A. Knyazev, G. I. Kropotov, K. N. Tykmakov, V. S. Pavelyev, E. V. Tsygankova, D. I. Tsypishka, and Yu. Yu. Choporova, Optical Memory and Neural Networks **23**, 185 (2014).
[32] V. Yu. Bazhenov, M. S. Soskin, and M. V. Vasnetsov, J. Mod. Opt. **39**, 985 (1992).
[33] H. I. Sztul and R. R. Alfano, Opt. Lett. **31**, 999 (2006).
[34] N. Yu and F. Capasso, Nat. Mater. **13**, 139 (2014).
[35] V. V. Gerasimov, V. S. Cherkassky, B. A. Knyazev, G. N. Kulipanov, I. A. Kotelnikov, A. K. Nikitin, and G. N. Zhizhin, J. Opt. Soc. Am. B **30**, 2182 (2013).
[36] H. Hu, X. Zeng, D. Ji, L. Zhu, and Q. J. Gan, J. Appl. Phys. **113**, 053101 (2013).
[37] I. A. Kotelnikov, V. V. Gerasimov, and B. A. Knyazev, Phys. Rev. A **87**, 023828 (2013).